

Stathmin/Op18 Phosphorylation Is Regulated by Microtubule Assembly

Thomas Küntziger,* Olivier Gavet,^{†‡} Valérie Manceau,[†] André Sobel,[†] and Michel Bornens*[§]

*Institut Curie, Section Recherche, Unité Mixte de Recherche 144 Centre National de la Recherche Scientifique, 75248 Paris Cedex 05, France; and [†]Institut National de la Santé et de la Recherche Médicale U440, Institut du Fer à Moulin, F-75005 Paris, France

Submitted July 3, 2000; Revised October 25, 2000; Accepted December 6, 2000
Monitoring Editor: J. Richard McIntosh

Stathmin/Op 18 is a microtubule (MT) dynamics-regulating protein that has been shown to have both catastrophe-promoting and tubulin-sequestering activities. The level of stathmin/Op18 phosphorylation was proved both in vitro and in vivo to be important in modulating its MT-destabilizing activity. To understand the in vivo regulation of stathmin/Op18 activity, we investigated whether MT assembly itself could control phosphorylation of stathmin/Op18 and thus its MT-destabilizing activity. We found that MT nucleation by centrosomes from *Xenopus* sperm or somatic cells and MT assembly promoted by dimethyl sulfoxide or paclitaxel induced stathmin/Op18 hyperphosphorylation in *Xenopus* egg extracts, leading to new stathmin/Op18 isoforms phosphorylated on Ser 16. The MT-dependent phosphorylation of stathmin/Op18 took place in interphase extracts as well, and was also observed in somatic cells. We show that the MT-dependent phosphorylation of stathmin/Op18 on Ser 16 is mediated by an activity associated to the MTs, and that it is responsible for the stathmin/Op18 hyperphosphorylation reported to be induced by the addition of "mitotic chromatin." Our results suggest the existence of a positive feedback loop, which could represent a novel mechanism contributing to MT network control.

INTRODUCTION

Stathmin/Op18, also known as p19, metablastin, and prosolin, is a cytosolic protein that is phosphorylated on up to four serine residues in response to the activation of various intracellular signaling pathways, in particular when triggered by extracellular signals (Sobel *et al.*, 1989). It was thus proposed to act as an intracellular relay integrating diverse signaling pathways (Sobel, 1991). Stathmin/Op18 was subsequently found to have a microtubule (MT) destabilizing activity (Belmont and Mitchison, 1996; Horwitz *et al.*, 1997; Jourdain *et al.*, 1997; Larsson *et al.*, 1997). The MT-destabilizing activity of stathmin/Op18 can be turned off in vivo by phosphorylation on its four serine residues (Horwitz *et al.*, 1997; Gavet *et al.*, 1998), and remarkably stathmin/Op18 is highly phosphorylated on all its four sites at mitosis (Strahler *et al.*, 1992; Brattsand *et al.*, 1994; Luo *et al.*, 1994; Gavet *et al.*, 1998). It has been shown that overexpression of wild-type phosphorylatable stathmin/Op18 in mammalian cells does not prevent spindle formation in mitosis, whereas overexpression of stathmin/Op18 with mutated nonphos-

phorylatable sites does (Marklund *et al.*, 1996; Gavet *et al.*, 1998). Thus, the MT-destabilizing activity of stathmin/Op18 is likely down-regulated by phosphorylation to allow formation of the mitotic spindle and progression through mitosis.

Two mechanisms, observed in vitro in a pH-dependent manner (Howell *et al.*, 1999b), have been proposed to explain the MT-destabilizing activity of stathmin/Op18. Stathmin/Op18 forms with free tubulin a sequestering T₂S complex in which one molecule of stathmin/Op18 binds two α/β -tubulin dimers (Curmi *et al.*, 1997; Jourdain *et al.*, 1997; Gigant *et al.*, 2000; Steinmetz *et al.*, 2000). This effect could explain its depolymerizing effect on MTs (Curmi *et al.*, 1997; Jourdain *et al.*, 1997; Howell *et al.*, 1999b; Larsson *et al.*, 1999; Gigant *et al.*, 2000; Steinmetz *et al.*, 2000) and make stathmin/Op18 the first identified tubulin-sequestering protein. Because the completely pseudophosphorylated form (in which the four phosphorylatable serine sites are mutated to glutamic acid) has a lower affinity for tubulin than the nonphosphorylated form and hence decreased sequestering activity, the observed down-regulation by phosphorylation of stathmin/Op18 activity on MTs could be explained this way (Curmi *et al.*, 1997; Jourdain *et al.*, 1997; Larsson *et al.*, 1997). Alternatively, stathmin/Op18 also increases the catastrophe frequency of MTs (Belmont and Mitchison, 1996; Howell *et al.*,

[†] Present address: Institut Curie, Section Recherche, UMR 144 CNRS, 26 rue d'Ulm, 75248 Paris Cedex 05, France.

[§] Corresponding author: E-mail address: mbornens@curie.fr.

1999a,b). Although one would expect a tubulin-sequestering protein to increase catastrophe frequency as a result of the decrease in the free tubulin concentration, part of the catastrophe-promoting activity of stathmin/Op18 is independent of its sequestering activity and could involve an interaction with MT extremities (Howell *et al.*, 1999b; Larsson *et al.*, 1999; Steinmetz *et al.*, 2000).

Because some kinases and phosphatases have been shown to be associated with MTs (Ohta *et al.*, 1990; Ookata *et al.*, 1993; Reszka *et al.*, 1995; Sontag *et al.*, 1995; Morishima-Kawashima and Kosik, 1996), and because examples of kinase activities regulated through phosphorylation following MT assembly have been reported (Shinohara-Gotoh *et al.*, 1991; Srivastava *et al.*, 1998), we wished to investigate whether MT assembly itself could regulate stathmin/Op18 activity by modulating its phosphorylation level. We found that MT nucleation by centrosomes from *Xenopus* sperm or somatic cells and MT assembly by paclitaxel, dimethyl sulfoxide (DMSO), or chromatin induced stathmin/Op18 hyperphosphorylation in *Xenopus* egg extracts. The responsible kinase activity was found to cosediment with assembled MTs and to lead to new stathmin/Op18 isoforms phosphorylated on Ser 16. The appearance of Ser 16-phosphorylated forms was detected very soon after MT assembly but hyperphosphorylation became maximal only after a significant lag. The MT-dependent phosphorylation of stathmin/Op18 took place in interphase extracts as well, and also in somatic cells. Altogether, our results suggest the existence of a positive feedback loop, which could represent a new, amplifying, mechanism for MT network control.

MATERIALS AND METHODS

Preparation of *Xenopus* Egg Extracts

Low-speed (15,000 × *g*) *Xenopus* egg extracts blocked in metaphase II of meiosis (cytostatic factor [CSF] extracts) and permeabilized sperm heads were prepared as described (Murray, 1991). High-speed extracts were prepared from CSF extracts spun at 245,000 × *g* for 20 min at 4°C in a TLS 55 rotor (Beckman, Palo Alto, CA) and were complemented with 1/20 volume of Energy Mix (150 mM creatine phosphate, 20 mM ATP, 20 mM MgCl₂). Interphase extracts were prepared from low-speed extracts activated with 0.4 mM Ca²⁺ and complemented with 200 μg/ml cycloheximide (Sigma, St. Louis, MO). H₁ kinase activity was measured as described (Murray, 1991). KE 37 cells isolated centrosomes were prepared as described (Bornens and Moudjou, 1999). Nuclei devoid of any cytoplasmic contaminant or of nuclear envelope, but containing the native distribution of perinuclear and perinucleolar condensed chromatin (Bornens, 1968), were obtained from KE 37 cells treated with 1% citric acid (Mirsky and Pollister, 1946). Each nucleus corresponds to a unit of chromatin.

HeLa Cell Extracts

HeLa cell synchronization and extract preparation were performed as in (Gaglio *et al.*, 1995). To synchronise at G₁ and G₂/M, cells synchronized in S were released from the second thymidine block for 11 and 7 h, respectively. Cells were then treated for 2 h before extracts were prepared with the MT-affecting drugs paclitaxel (1 μM) and nocodazole (1 μM).

Microtubule Polymerization

Extracts were incubated for a variable amount of time at 22°C with DMSO (5%; ICN, Costa Mesa, CA), paclitaxel (0.1 μM; Rhône-

Poulenc Rorer, Vitry-sur Seine, France), sperm heads (2 × 10³/μL extract), centrosomes (2 × 10³/μL extract), nuclei (between 7.5 × 10³ and 1.1 × 10⁴ units of chromatin/μL extract), or nocodazole (10 μM; Sigma). High-speed extracts were layered on top of a BRB80 (80 mM K-piperazine-N,N'-bis(2-ethanesulfonic acid), pH 6.8, 1 mM MgCl₂, 1 mM EGTA)/40% glycerol cushion containing 10 μg/ml protease inhibitors: leupeptin, pepstatin, and chymostatin (Boehringer, Mannheim, Germany). Centrifugation was at 22°C for 20 min at 140,000 × *g* in a TLS 55 rotor (Beckman). A sample from the supernatant was taken and the remaining volume discarded, the pellet washed once with BRB80, and left to dry before an equal volume of buffer A (Laemmli, 1970) was added to both supernatant and pellet fractions. An equal fraction in volume of both samples was loaded for 12% SDS-PAGE.

Antibodies

Stathmin/Op18 antibodies (both sera and affinity-purified) were polyclonal anti-COOH-terminal (C) and anti-internal (I) peptides of human stathmin/Op18. Antibody C was thus specific of the human form of stathmin/Op18, whereas antibody I recognized both human and *Xenopus* forms of stathmin/Op18 (Koppel *et al.*, 1990). Rabbit polyclonal antiphosphorylated serine 16 (Gavet *et al.*, 1998) was generated against the [Y-L-E-K-R-A-S(PO₃H₂)-G-Q-A-F-E] peptide conjugated to KLH (Neosystem, Strasbourg, France). Monoclonal anti-α-tubulin was from Amersham (Little Chalfont, England), and polyclonal anti-γ-tubulin is described in Moudjou *et al.* (1996).

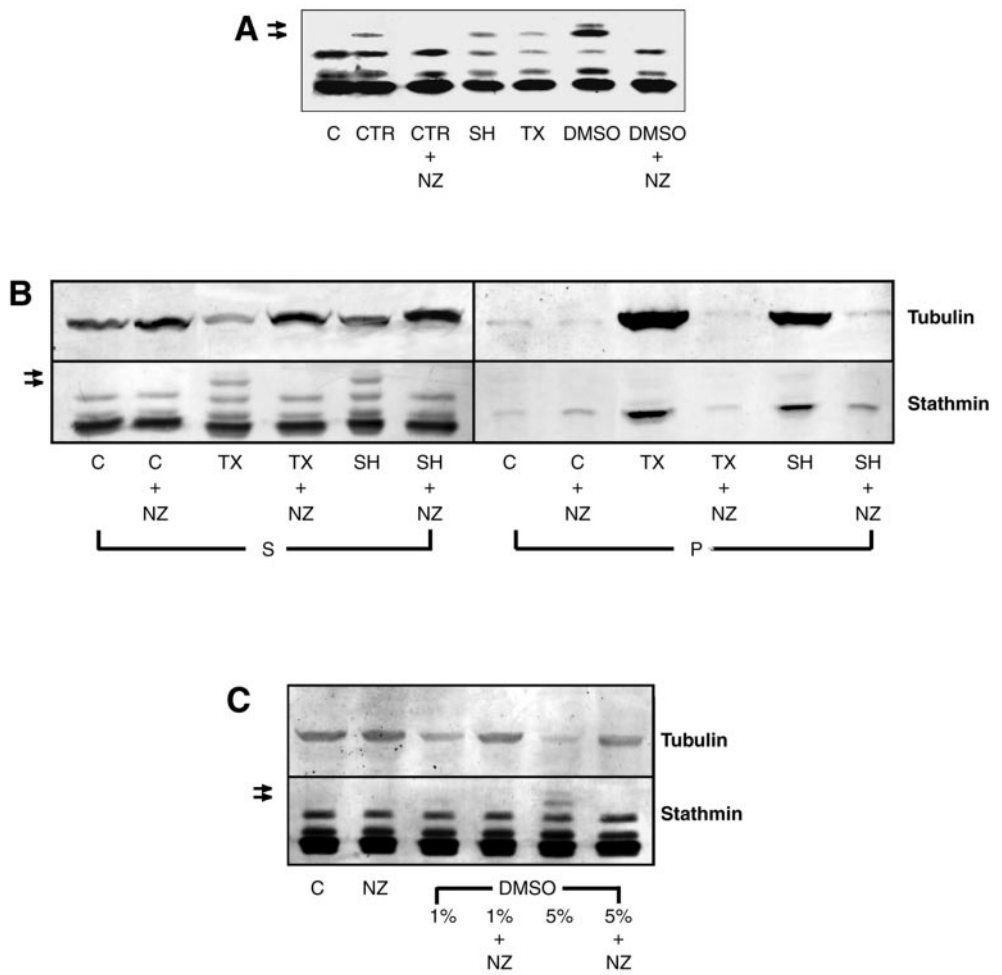
Two-dimensional Gel Analysis

Two-dimensional gels were performed as described in Sobel and Tashjian (1983): the isoelectric focusing gel contained ampholines pH 5–8 (HeLa cell extracts) or pH 5–9 (*Xenopus* egg extracts), and the second dimension was run on 12.5% SDS polyacrylamide gels. Proteins were transferred to nitrocellulose with a semidry electroblotting apparatus, in a buffer containing 48 mM Tris, 39 mM glycine, and 20% isopropanol. Proteins were further fixed with 0.25% glutaraldehyde at room temperature for 20 min. Membranes were blocked with 5% dry milk in Tris-buffered saline/Tween 20 buffer (12 mM Tris-HCl pH 7.4, 160 mM NaCl, 0.1% Triton X-100) and probed for 1 h with diluted primary antibodies in Tris-buffered saline/Tween 20. The following primary antibody dilutions were used: serum I, 1:10,000; serum C, 1:20,000; anti-Ser 16P, 1:300,000; and anti-α-tubulin, 1:200. Bound antibodies were detected by anti-rabbit or anti-mouse antibodies coupled to peroxidase (1:5000; Dako, Carpinteria, CA) and revealed by the enhanced chemiluminescence kit protocol (Amersham). For monodimensional Western blots, secondary antibodies coupled to alkaline phosphatase were used (1:7500; Promega, Madison, WI).

Quantitation

Absolute quantitation of the amount of stathmin/Op18 phosphorylated following MT assembly was performed on two-dimensional Western blots from three different experiments using DMSO as the polymerizing agent. Antiserum I was used as the primary antibody, and ³⁵S-labeled-anti-rabbit IgG (Amersham) was used as the secondary antibody. A control extract in which MT assembly was not induced was used to delimit the spots corresponding to MT-dependent phosphorylation. The radioactive disintegrations were recorded over 4 d with an InstantImager (Packard, Meriden, CT), and the sum of the four major spots corresponding to MT-dependent phosphorylation was expressed as a ratio of total stathmin/Op18. In Figures 5 and 8, relative quantitations were performed to monitor the evolution of phosphorylation on Ser 16 by using Image Quant version 4.2 software (Molecular Dynamics, Sunnyvale, CA) on scanned Western blots revealed with alkaline phosphatase. To control for differences in the amount of proteins loaded, an internal standard was used in each lane: the amount of phosphorylation on

Figure 1. MT assembly induces stathmin/Op18 hyperphosphorylation in mitotic *Xenopus* egg extracts. (A) Stathmin/Op18 phosphorylation pattern (probed with antistathmin/Op18 serum I) in low-speed mitotic *Xenopus* egg extracts in the absence (C, control) or presence of MT-nucleating structures (CTR, somatic centrosomes, $2 \times 10^3/\mu\text{l}$ extract; SH, sperm heads, $2 \times 10^3/\mu\text{l}$ extract) or assembly-promoting agents (TX, paclitaxel, $0.1 \mu\text{M}$; DMSO, 5%). Nocodazole (NZ, $10 \mu\text{M}$) was added in some conditions to prevent MT assembly. MT-dependent hyperphosphorylated forms of stathmin/Op18 are indicated by arrows. (B) Stathmin/Op18 phosphorylation and tubulin distribution in supernatant (S) and pellet (P) of high-speed mitotic *Xenopus* egg extract after MT polymerization. In all cases, comparative aliquots of both fractions were separated on 12% polyacrylamide gels, and further processed for immunodetection with anti-stathmin/Op18 and anti-tubulin antibodies (MT-dependent hyperphosphorylated forms of stathmin/Op18 are indicated by arrows). (C) Stathmin/Op18 hyperphosphorylation pattern and tubulin content of high-speed extract supernatant in which 1 or 5% DMSO was added. (MT-dependent hyperphosphorylated forms of stathmin/Op18 are indicated by arrows.) In each case, no stathmin/Op18 hyperphosphorylation was detected in nocodazole-containing conditions, even with longer revelation. The patterns shown are representative for each series of at least three experiments leading to similar results.



Ser 16 in supernatants is presented as a ratio to the total amount of stathmin/Op18.

Fractionation of the Stathmin/Op18 Phosphorylating Activity

Mitotic *Xenopus* high-speed extracts were incubated for 45 min at 22°C with 5% DMSO, and 10^{-5} M nocodazole in some conditions. MTs were pelleted as described above and resuspended in BRB 80/40% glycerol containing protease inhibitors and 1 mM ATP (Boehringer). A four-time excess of human wild-type stathmin/Op18 and [γ - ^{32}P] ATP ($0.5 \mu\text{Ci}/\mu\text{l}$ extract) was added to an equal volume of supernatant and pellet fractions and left to incubate for 15 min at room temperature. An equal volume of buffer A was added to both S and P fractions, and the same amount was loaded on 12% acrylamide gels for Western blot analysis and autoradiography (Phosphorimager Storm 860; Molecular Dynamics).

RESULTS

Hyperphosphorylation of Stathmin/Op18 in the Presence of Polymerized Microtubules

Low-speed ($15,000 \times g$) mitotic CSF-arrested *Xenopus* egg extract (Sawin and Mitchison, 1991) was incubated for 45

min at 22°C in the presence of various factors able to promote MT assembly. We used *Xenopus* sperm heads and isolated human somatic centrosomes, which both induce MT nucleation, and two agents able to promote MT polymerization and aster formation by different mechanisms: paclitaxel (Taxol, 10^{-7} M), which binds to MTs, and DMSO (5%), which acts through a solvent-based mechanism. In all cases, one or two bands with reduced electrophoretic mobilities and representing hyperphosphorylated forms of stathmin/Op18 (Beretta *et al.*, 1993; see below) were observed by Western blot (Figure 1A). These were in addition to the triplet of bands observed in the control extract and which correspond to the nonphosphorylated and diverse phosphorylated forms of *Xenopus* stathmin/Op18 (Maucuer *et al.*, 1993; Andersen *et al.*, 1997). The hyperphosphorylated forms were no longer present when incubations were carried out in the presence of 10^{-5} M nocodazole to prevent MT polymerization. From these results we conclude that the presence of hyperphosphorylated forms of stathmin/Op18 is, in part, a MT assembly-dependent phenomenon.

Similar results were obtained with high-speed ($245,000 \times g$) mitotic *Xenopus* egg extracts that were incubated for 45

min in the presence of either *Xenopus* sperm heads or paclitaxel before MTs were pelleted by ultracentrifugation. The pattern of stathmin/Op18 phosphorylation in the MT pellet and in the supernatant was analyzed by Western blot, as well as the tubulin distribution between the two fractions (Figure 1B). As expected, the presence of sperm heads and paclitaxel increased the level of polymerized tubulin in the pellet. Stathmin/Op18 remained essentially in the soluble fraction but a small fraction sedimented with the MT pellet, possibly representing a minor MT-associated stathmin/Op18 pool. The additional hyperphosphorylated forms of stathmin/Op18 found in the presence of paclitaxel and sperm heads were only observed in the supernatant fraction. They were no longer observed if nocodazole was added to the extract together with sperm heads or paclitaxel, confirming that regulation of stathmin/Op18 phosphorylation in high-speed *Xenopus* egg extracts is at least partially a MT assembly-dependent phenomenon.

Among all the MT-promoting agents used, DMSO (5%) had the strongest effect in terms of stathmin/Op18 hyperphosphorylation (Figure 1A). This correlates with a significant increase in the amount of polymerized tubulin as can be seen by the almost complete absence of tubulin in the corresponding supernatant (Figure 1C). This effect on the phosphorylation pattern of stathmin/Op18 was again abolished if nocodazole was added together with 5% DMSO. On the other hand, the presence of 1% DMSO in high-speed *Xenopus* egg extracts did not result in a significant increase of stathmin/Op18 phosphorylation, and there was only a moderate decrease in the quantity of tubulin in the supernatant compared with a control extract.

To confirm the existence of a particular phosphorylation pattern of stathmin/Op18 resulting from MT assembly, supernatants from high-speed *Xenopus* egg extracts incubated for 45 min with either paclitaxel, *Xenopus* sperm heads, or DMSO were submitted to two-dimensional Western blot analysis (Figure 2). In all cases where MT assembly was induced, four additional spots (arrowheads) corresponding to highly phosphorylated isoforms could be detected compared with a control extract showing the typical phosphorylation pattern of *Xenopus* stathmin/Op18 (Maucuer *et al.*, 1993). The intensity of the additional spots was higher with DMSO, and they were abolished in all cases in the presence of nocodazole. We conclude from these results that the assembly of MTs in *Xenopus* egg extracts provokes the appearance of newly phosphorylated stathmin/Op18 isoforms.

The stathmin/Op18 phosphorylation pattern on two-dimensional Western blots allows separation of isoforms phosphorylated in an MT-dependent way. To quantify the amount of MT-dependent phosphorylation, we used a radiolabeled secondary antibody on two-dimensional blots following MT assembly with 5% DMSO from three independent experiments. In each case, we summed the radioactive disintegrations corresponding to the clearly distinguishable MT-dependent spots (compared with the phosphorylation pattern of an extract where no MT assembly had been induced). MT-dependent phosphorylation was found to represent 9.9, 3.8, and 11.3% of total stathmin/Op18, depending on the extract, with a mean value of 8.3%, the observed differences arising from the variability inherent to *Xenopus* egg extracts.

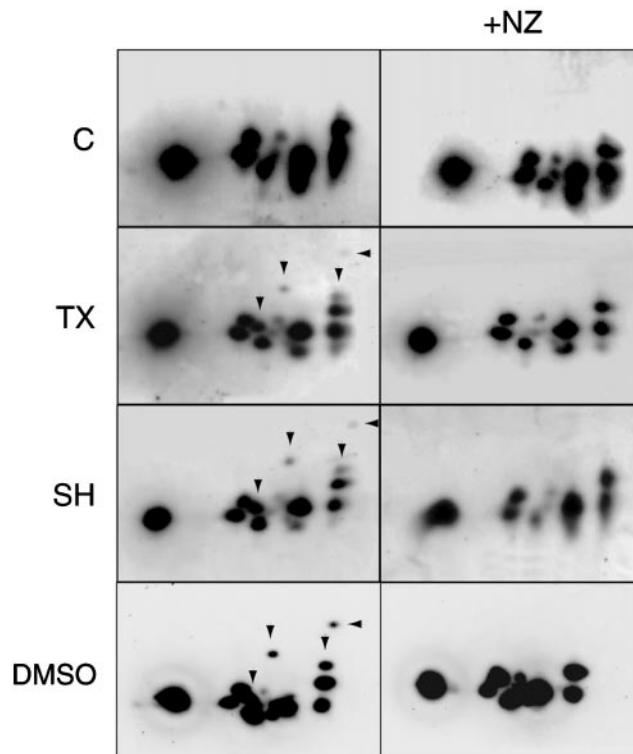
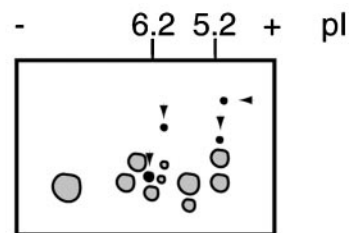


Figure 2. MT assembly results in at least four major specific phosphorylated stathmin/Op18 forms. Two-dimensional gel analysis of high-speed mitotic *Xenopus* egg extract supernatants (immunoblots probed with antiserum I) shows four extra spots (arrowheads) in conditions where MT assembly was induced (TX, SH, DMSO). These spots were absent in the same conditions with 10 μ M NZ (right). Schematic representation of the stathmin/Op18 phosphorylation pattern: spots present in control and nocodazole-containing fractions are gray, the additional spots induced by MT assembly are black.

Microtubule-dependent Phosphorylation of Stathmin/Op18 in Interphase

To determine whether the MT-induced phosphorylation of stathmin/Op18 is dependent on the presence of active mitosis promoting factor (MPF) in the extract or could take place in interphase, we drove high-speed mitotic extracts into interphase with 0.4 mM Ca^{2+} in the presence of cycloheximide (200 $\mu\text{g}/\text{ml}$), to prevent return to mitosis by endogenous synthesis of mitotic cyclins (Sawin and Mitchison, 1991). Thirty minutes after Ca^{2+} addition, extracts were

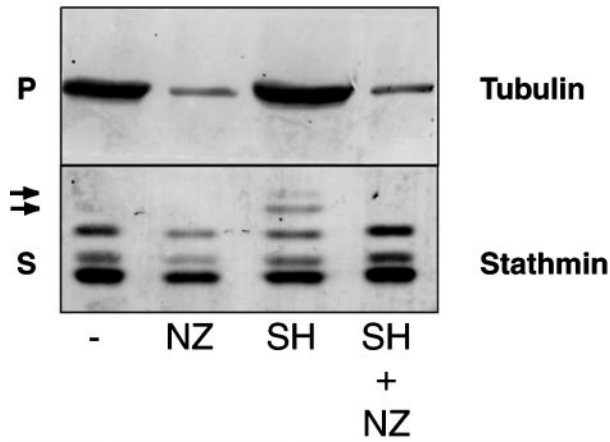


Figure 3. MT-dependent phosphorylation of stathmin/Op18 in interphase. *Xenopus* high-speed CSF-arrested egg extract was shifted to interphase by addition of 0.4 mM Ca²⁺ for 30 min before addition of cycloheximide (CHX) to maintain interphase state during 45 min. When indicated, sperm heads (SH) and NZ were added with CHX. Supernatants (S) were probed with antibody I and pellets (P) with anti- α -tubulin. MT-dependent hyperphosphorylated forms of stathmin/Op18 are indicated by arrows. The tubulin pellet found in control conditions (lane -) results from autopolymerization common in interphase egg extracts. The absence of a corresponding stathmin/Op18 hyperphosphorylation could be due to a different organization of the microtubules (see DISCUSSION).

incubated with *Xenopus* sperm heads for 45 min and separated between pellet and supernatant before analysis of stathmin/Op18 and tubulin by Western blot. As shown in Figure 3, *Xenopus* sperm heads induced polymerization of MTs, resulting in the hyperphosphorylation of stathmin/Op18. The intensity of the bands representing hyperphosphorylated forms was often reduced compared with those observed in a mitotic extract (our unpublished results). As a control, stathmin/Op18 hyperphosphorylation was not observed when MT polymerization was prevented by nocodazole addition. We therefore conclude that the phosphorylation of stathmin/Op18 in response to MT polymerization is at least partially independent of p34^{cdc2} activity.

Phosphorylation of Stathmin/Op18 on Ser 16

We wished to investigate which of the phosphorylation sites of *Xenopus* stathmin/Op18 (namely, Ser 16, 25, and 39) was implicated in its MT-dependent phosphorylation. Because the phosphorylation of serine 16 is known to be critical in the regulation of stathmin/Op18 MT-depolymerizing activity (Melander Gradin *et al.*, 1997; Gavet *et al.*, 1998), an anti-16P antiserum directed specifically against the phosphorylated Ser 16 of stathmin/Op18 (Gavet *et al.*, 1998) was used on two-dimensional blots of *Xenopus* high-speed extracts in which MT assembly had been promoted. As can be seen on Figure 4, the four spots associated with MT assembly in sperm heads, paclitaxel, and DMSO-containing extracts (Figure 2) were recognized by the anti-16P antiserum. No immunoreactive spot was detected in a control extract as well as in extracts treated with nocodazole, in contrast with the pattern observed when using an antibody recognizing all

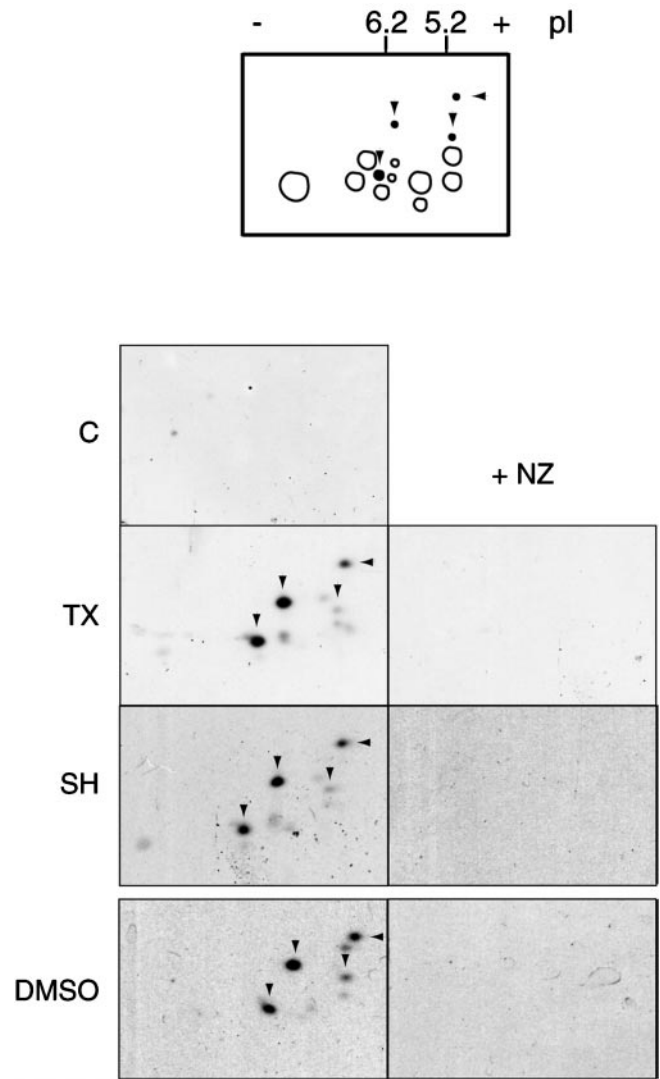


Figure 4. MT assembly-dependent phosphorylation on Ser 16. Two-dimensional immunoblots of *Xenopus* high-speed mitotic egg extracts probed with antiphosphorylated Ser 16 stathmin/Op18 antiserum (anti-Ser16P). In all conditions where MTs were allowed to polymerize for 45 min, four main spots (arrowheads) corresponding to hyperphosphorylated isoforms revealed by antiserum I were detected (Figure 2). Several other minor spots were detected as well. They were not observed when nocodazole (NZ) was present. Schematic representation of the total stathmin/Op18 phosphorylation pattern as found in Figure 2 is shown on top: the additional spots induced by MT assembly and recognized by anti-Ser16P are black and pointed by arrowheads; spots present in control and nocodazole-containing fractions are not recognized by anti-Ser16P.

forms of stathmin/Op18 (Figure 2). Therefore, in the control extract these forms correspond to nonphosphorylated stathmin/Op18 or to stathmin/Op18 phosphorylated on different combination of sites but not on Ser 16. Our finding that MT assembly provokes phosphorylation of stathmin/Op18 on Ser 16 is consistent with the hyperphosphorylated forms of stathmin/Op18 observed in one-dimensional gel analysis (Figure 1), because phosphorylation on Ser 16 of mammalian

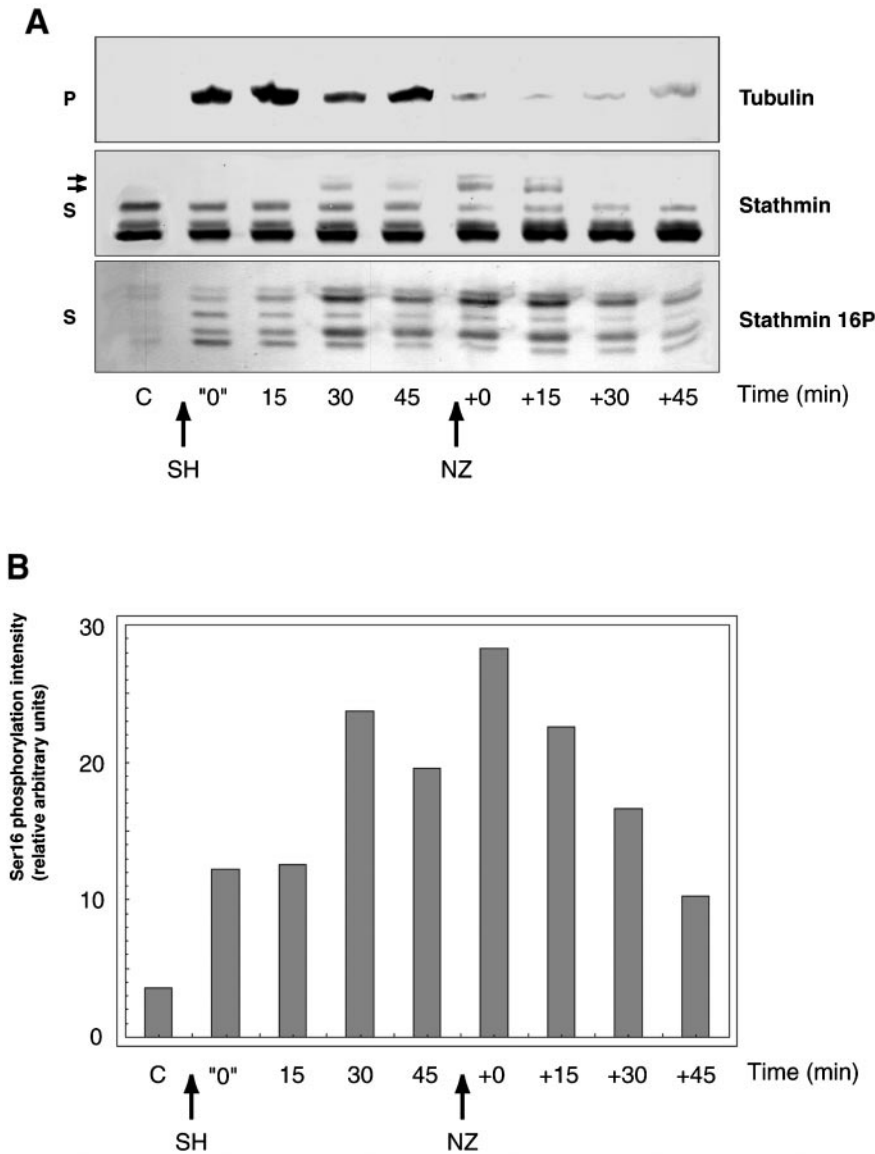


Figure 5. Stathmin/Op18 hyperphosphorylation results from MT assembly and becomes maximal after a significant lag. (A) SH-induced tubulin polymerization at 22°C in high-speed mitotic *Xenopus* egg extract results in the immediate phosphorylation of stathmin/Op18 on Ser 16 (stathmin 16P), and hyperphosphorylation becomes maximal between 15 and 30 min (stathmin and stathmin 16P). Repeated experiments show this lag to be closer to 15 min. After 45 min, addition of NZ results in rapid MT depolymerization, as judged by the decrease in the amount of tubulin in the pellet (P), and the slow disappearance of the hyperphosphorylated isoforms of stathmin/Op18 after ~15 min in the supernatant (S, see arrows). (B) Graph showing the intensity of the bands corresponding to phosphorylation on stathmin/Op18 Ser 16 in A (stathmin 16P). Results are expressed for each lane as a ratio of phosphorylation on Ser 16 (stathmin 16P) to total stathmin/Op18 (stathmin) that remains constant throughout the experiment and thus represents an internal control.

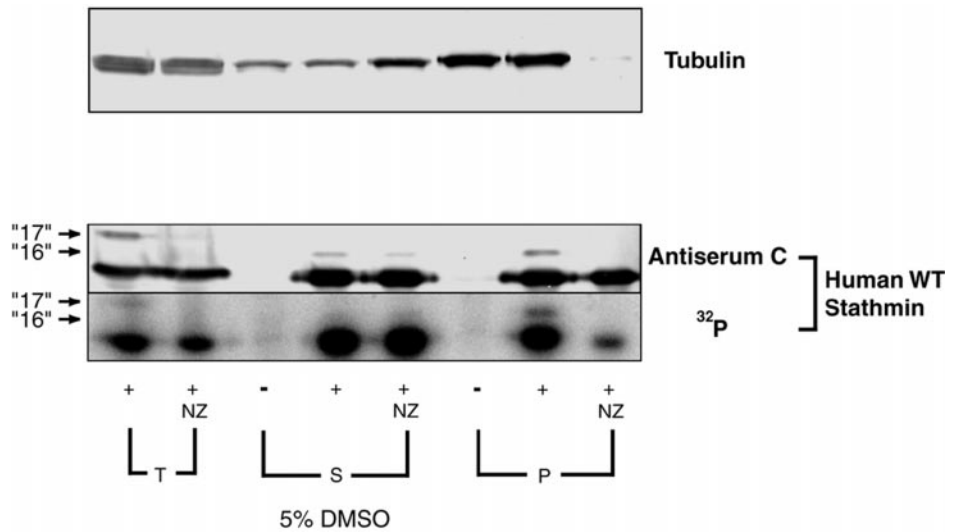
stathmin/Op18 is required to generate isoforms with reduced electrophoretic mobilities (Beretta *et al.*, 1993). One cannot exclude however that MT polymerization might result in the phosphorylation of stathmin/Op18 on other sites as well. Taken together, these results show that assembling MTs leads to the phosphorylation on Ser 16 of stathmin/Op18, which was not phosphorylated on that particular site before MT assembly.

Mechanism of Microtubule-dependent Stathmin/Op18 Phosphorylation

To characterize the mechanism of stathmin/Op18 hyperphosphorylation, we compared the time courses of MT polymerization and stathmin/Op18 phosphorylation. Mitotic high-speed extracts were incubated for different time points at 22°C with *Xenopus* sperm heads and were then centri-

fuged to separate MTs from unpolymerized tubulin. The respective kinetics of MT polymerization, stathmin/Op18 global phosphorylation (Figure 5A, stathmin) and Ser 16 specific phosphorylation (Figure 5A, stathmin 16P) were monitored by Western blot. After 45 min, 10⁻⁵ M nocodazole was added and the evolution of tubulin in pellets and stathmin/Op18 phosphorylation in supernatants was again monitored by Western blot. The effect of *Xenopus* sperm heads on MT polymerization was so rapid that it was even visible at time zero (Figure 5A, P-tubulin), indicating that it was taking place during the beginning of centrifugation. Phosphorylation on Ser 16 was detected as soon as sperm heads were added (Figure 5A, S-stathmin 16P), but the intensity of the two upper bands corresponding to the hyperphosphorylated forms of stathmin/Op18 gradually increased and became maximal after a 15- to 30-min lag.

Figure 6. The MT-dependent phosphorylating activity cosediments with MTs. Phosphorylation of human stathmin/Op18 in total (T), supernatant (S), and pellet (P) of high-speed mitotic *Xenopus* egg extracts. Extract aliquots were incubated for 45 min with 5% DMSO alone (+) or with 10 μ M NZ (+NZ), then centrifuged to separate MTs from soluble tubulin. [γ - 32 P] ATP and recombinant human wild-type stathmin/Op18 were added to equal volumes of total, supernatant and resuspended pellet fractions which were incubated for 15 min at room temperature (control samples with no human stathmin/Op18 added are indicated by -). Tubulin was revealed by immunodetection. Human stathmin/Op18 was either specifically revealed by antiserum C (which does not cross-react with *Xenopus* stathmin/Op18), or by autoradiography (32 P). Arrows point to hyperphosphorylated human forms "16" and "17."



Accordingly, the hyperphosphorylated stathmin/Op18 forms accumulated over time and only became detectable with the anti-stathmin antibody after the same lag of 15 to 30 min (Figure 5A, S-stathmin). This was confirmed by monitoring the variations in Ser 16 phosphorylation by densitometry, by using total stathmin/Op18 as an internal standard (Figure 5B). After nocodazole addition, MT depolymerization was visible at time zero in pellets, whereas another gap of more than 15 min was required to observe the disappearance of the hyperphosphorylated forms (Figure 5A, S-stathmin) and a progressive decrease in stathmin/Op18 phosphorylation on Ser 16 (Figure 5A, S-stathmin 16P; and B). This shows that although phosphorylation on stathmin/Op18 Ser 16 starts immediately upon MT assembly, a longer period of more than 15 min is required to reach an equilibrium situation in which stathmin/Op18 hyperphosphorylation is maximal.

At this stage, two hypotheses could be considered to explain the MT-dependent phosphorylation of stathmin/Op18. MT assembly would displace the tubulin equilibrium between free and stathmin/Op18-bound forms toward the free form, thus enabling liberation and phosphorylation of stathmin/Op18 by kinases present in the extract (assuming that phosphorylation on stathmin/Op18 is increased on the unbound form). In that case, however, one should only expect an increase in the amount of the same phosphorylated stathmin/Op18 forms found in a control extract, but not the observed appearance of newly phosphorylated forms (Figure 1). The data rather argues for an MT assembly-dependent process that would trigger a change in the balance between kinase and phosphatase activities in the extract. To characterize the activity responsible for stathmin/Op18 phosphorylation following MT assembly, high-speed *Xenopus* egg extracts were incubated with 5% DMSO for 45 min at 22°C. One aliquot representing total extract (T) was kept, and the remaining extract was fractionated between supernatant (S) and pellet (P). A fourfold excess (relative to the endogenous *Xenopus* stathmin/Op18) of non-phosphorylated recombinant human stathmin/Op18 was then added to all fractions together with [γ - 32 P] ATP for 15

min at room temperature. As a control, we added nocodazole together with DMSO to the extract to prevent any tubulin polymerization. Recombinant human stathmin/Op18, which can be distinguished from endogenous *Xenopus* stathmin/Op18 by the use of antiserum C (Koppel *et al.*, 1990), and tubulin were analyzed by Western blot and by autoradiography. Significant hyperphosphorylation (band "16," phosphorylated on serine 16 and 25; Beretta *et al.*, 1993) of human stathmin/Op18 was observed in supernatant and pellet fractions (Figure 6), but only in the pellet was it found to be MT-dependent because it was not observed in the corresponding nocodazole-containing extract. Presence of nocodazole did not modify the phosphorylation activity in the supernatant. In total extract, a slower migrating band representing stathmin/Op18 phosphorylated on one additional site (band "17," phosphorylated on serine 16, 25, and 38; Beretta *et al.*, 1993) was present, suggesting that fractionating the extract resulted in fractionating the kinase/phosphatase activities required for phosphorylation on serine 16, 25, and 38. From this we conclude that the enzyme responsible for stathmin/Op18 phosphorylation in response to MT assembly sediments with the MT pellet.

MT-dependent Phosphorylation of Stathmin/Op18 in Somatic Cells

We then wanted to determine whether the MT-dependent phosphorylation of stathmin/Op18 was peculiar to embryonic systems or whether it could also be observed in somatic cells. To address this question, HeLa cells were synchronized in the G₁, S, and G₂/M stages of the cell cycle and then treated for 2 h with either paclitaxel or nocodazole. The phosphorylation pattern of human stathmin/Op18 was then analyzed by two-dimensional immunoblots. We observed, as reported previously (Strahler *et al.*, 1992; Luo *et al.*, 1994; Gavet *et al.*, 1998), the global increase in the phosphorylation of stathmin/Op18 as cells progress toward mitosis (Figure 7). Treatment with paclitaxel in G₁ and S led to cells with slightly more phosphorylated forms of stathmin/Op18 (arrowheads) compared with control cells, which confirms the

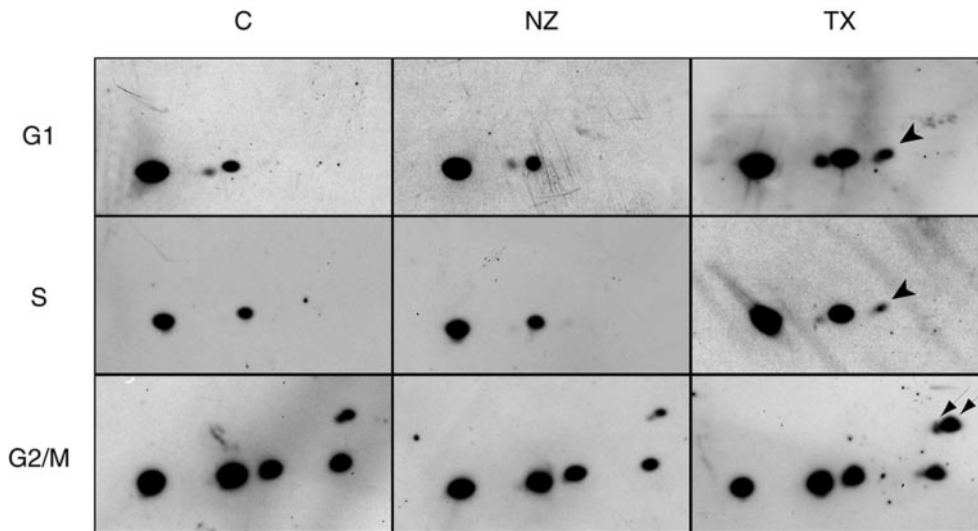


Figure 7. MT-dependent phosphorylation of stathmin/Op18 in somatic cells. Two-dimensional gel analysis of proteins from HeLa cells synchronised in G₁, S, and G₂/M phases were performed in control cells (C), or after 2 h treatment with paclitaxel (TX) or nocodazole (NZ). Proteins were further analyzed for stathmin/Op18 by immunoblotting with antiserum I. Large arrowheads point to an apparently more abundant hyperphosphorylated form in TX-treated G₁ and S cells. Small arrows point to more abundant tri- and tetraphosphorylated isoforms in TX-treated G₂/M cells.

effect observed in *Xenopus* interphase extracts (Figure 3). In G₂/M phase, stathmin/Op18 phosphorylation increased dramatically because the mitotic kinases are activated (Brattsand *et al.*, 1994). Furthermore, in paclitaxel-treated cells, the spots corresponding to tri- and tetraphosphorylated forms (arrows) were significantly increased compared with control cells or cells treated with nocodazole. These spots correspond to phospho-isomers phosphorylated on Ser 16 (Gavet *et al.*, 1998). This indicates that, as in embryonic systems, stathmin/Op18 hyperphosphorylation is in part dependent of MT assembly.

MT-dependent and Nuclei-induced Stathmin/Op18 Phosphorylation

To evaluate the significance of the MT-dependent phosphorylation of stathmin/Op18, we wished to examine its involvement in a physiological cell process. In *Xenopus* egg extracts, stathmin/Op18 hyperphosphorylation has been reported following the addition of "mitotic chromatin beads" and was proposed to contribute to the formation of spindles by locally enhancing MT stability around chromatin (Andersen *et al.*, 1997). We wondered whether chromatin-induced phosphorylation of stathmin/Op18 could be an indirect effect due to stabilization of MTs by the mitotic chromatin beads. We therefore used nuclei from somatic cells treated with citric acid (Mirsky and Pollister, 1946), which have been shown to be devoid of nuclear envelope and of centrosomes (Bornens, 1968; Figure 8B, γ -tubulin staining) and can therefore be considered as units of chromatin (see MATERIALS AND METHODS). We incubated them for 1 h in a high-speed mitotic *Xenopus* egg extract at several concentrations (from C1: 7.5×10^3 nuclei/ μ l to C3: 1.1×10^4 nuclei/ μ l) corresponding to the physiological DNA/cytoplasm ratio in an egg. We observed MTs in the vicinity of chromatin (Figure 8B). Analysis of the stathmin/Op18 phosphorylation pattern, of phosphorylation on Ser 16 in supernatants, and of tubulin in pellets (Figure 8A) showed that chromatin induced MT assembly and stathmin/Op18 hyperphosphorylation as well as phosphoryla-

tion on Ser 16. For each of the chromatin concentration tested, stathmin/Op18 hyperphosphorylation or phosphorylation on Ser 16 (Figure 8A) was no longer observed if MT assembly was prevented by nocodazole (see also the evolution of Ser 16 phosphorylation, Figure 8C). Quantitation of H₁ kinase activity (Figure 8D) showed that chromatin addition, just like for sperm heads, did not convert the mitotic extract into an interphase one. Altogether, this shows that the chromatin-promoted phosphorylation of stathmin/Op18 is actually due to the MT assembly induced by chromatin and not due to chromatin itself.

DISCUSSION

MT-dependent Regulation of Stathmin/Op18 Phosphorylation

The importance of the phosphorylation-dependent MT-depolymerizing activity of stathmin/Op18 is now well established (Horwitz *et al.*, 1997; Larsson *et al.*, 1997; Gavet *et al.*, 1998; Lawler *et al.*, 1998). Its down-regulation by phosphorylation has been shown to be indispensable for cells to progress through mitosis (Marklund *et al.*, 1996; Gavet *et al.*, 1998). Here, we present evidence that changing the level of MT polymerization induces the phosphorylation of stathmin/Op18 on at least one specific site (Ser 16), which is essential for regulating its activity on MTs (Melander Gradin *et al.*, 1997). Two mechanisms, catastrophe promotion (Belmont and Mitchison, 1996; Howell *et al.*, 1999b) and tubulin sequestration (Curmi *et al.*, 1997; Jourdain *et al.*, 1997; Gigant *et al.*, 2000), have been proposed to explain the effect on MT assembly by stathmin/Op18 observed *in vivo*. Even though our results do not provide direct evidence to privilege one mechanism rather than the other, the *in vivo* observed down-regulation of stathmin/Op18 activity by phosphorylation could be explained by the decreased sequestering activity of the tetraphosphorylated stathmin/Op18 (Curmi *et al.*, 1997; Jourdain *et al.*, 1997; Larsson *et al.*, 1997). On the other hand, the limited amount of stathmin/Op18 undergoing MT-dependent phosphorylation (~8% with DMSO), as-

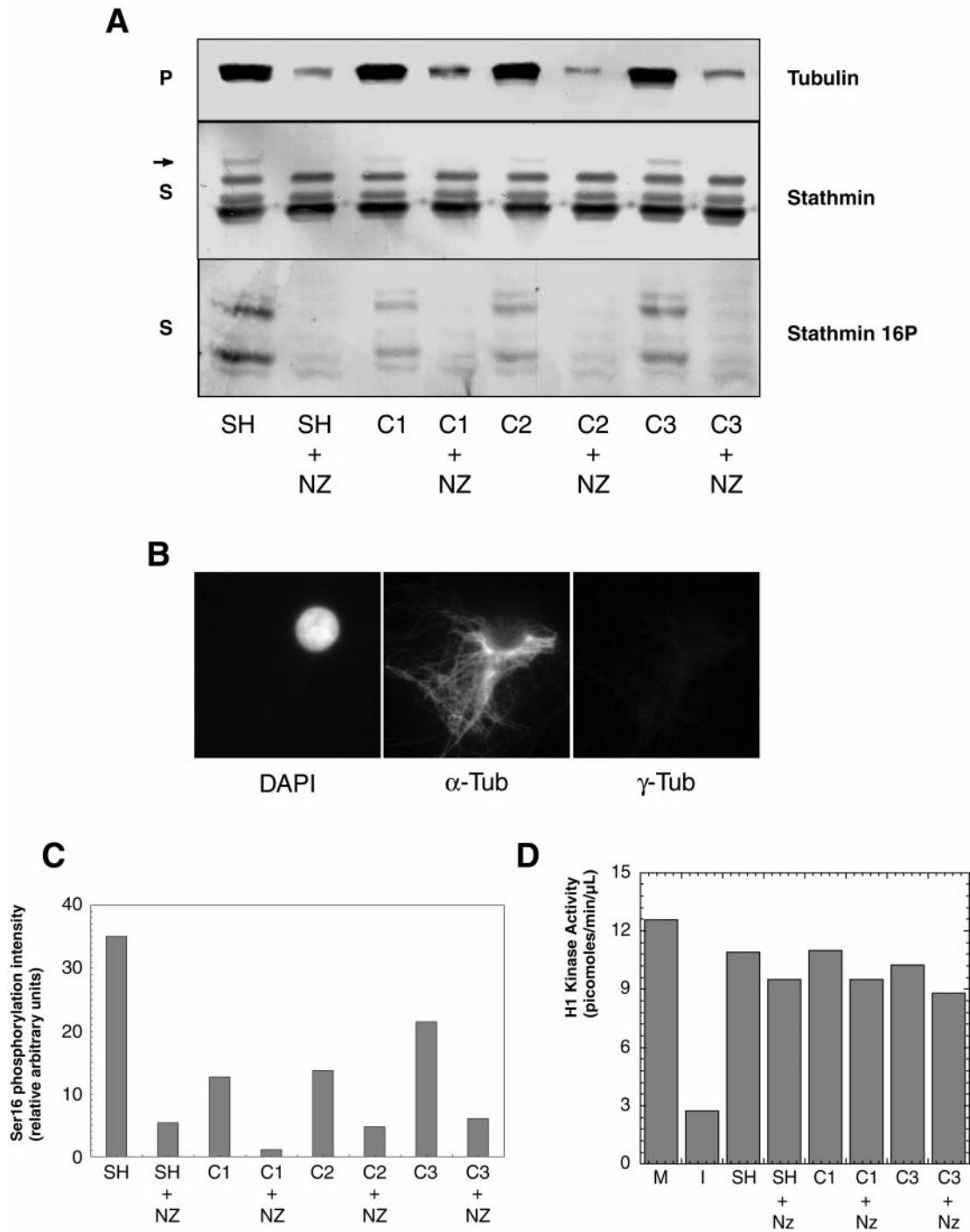


Figure 8. Nuclei induce stathmin/Op18 hyperphosphorylation through MT assembly. (A) Stathmin/Op18 phosphorylation pattern in supernatants (S) and tubulin distribution in pellets (P) of high-speed mitotic extracts after addition of sperm heads (SH) or nuclei at various concentrations (C1: 7.5×10^3 ; C2: 9×10^3 ; C3: 1.1×10^4 in nuclei/ μ L), with or without nocodazole (NZ). The MT-dependent hyperphosphorylated forms of stathmin/Op18 are indicated by arrows (the upper band is visible on the original Western blot). (B) Immunofluorescence analysis of citric acid nuclei added to high-speed mitotic *Xenopus* egg extracts. Nuclei are visualized with DAPI and MTs are assembled around chromatin in the absence of centrosomes. α -tub, anti- α -tubulin antibody; γ -tub, anti- γ -tubulin antibody. (C) Graph showing the intensity of the bands corresponding to phosphorylation on stathmin/Op18 Ser 16 in A (stathmin 16P). Results are expressed for each lane as a ratio of phosphorylation on Ser 16 (stathmin 16P) to total stathmin/Op18 (stathmin), which remains constant throughout the experiment and thus represents an internal control. (D) H₁ kinase activity quantitation of extracts to which sperm heads or nuclei was added, in the absence or presence of nocodazole (NZ). In neither case was the original mitotic extract (M) shifted to interphase, as happens when calcium (0.4 mM) is added (I).

suming it modulates the catastrophe activity, would become physiologically more relevant as catastrophe promotion would be a highly substoichiometric mechanism.

Our finding that MT assembly can result in phosphorylation of a soluble target is not surprising when one considers that many kinases and phosphatases, such as mitogen-activated protein (MAP) kinase (Reszka *et al.*, 1995; Morishima-Kawashima *et al.*, 1996), p34^{cdc2} (Ookata *et al.*, 1993), Ca²⁺/calmodulin-dependent protein kinase II (Ohta *et al.*, 1990), and PP2A (Sontag *et al.*, 1995) are associated with MTs. These are also known to be effectors of stathmin/Op18 phosphorylation *in vitro* (Beretta *et al.*, 1993; Tournebize *et al.*, 1997; le Gouvello *et al.*, 1998), and interestingly some kinases are activated in response to a change in the cellular MT network. For example, MT disruption by colchicine or vinblastine in rat fibroblastic cells results in MAP kinase activation (Shinohara-Gotoh *et al.*, 1991), and it was shown that treatment of human breast cancer cells with paclitaxel or vincristine (an MT-disrupting agent) induces protein kinase A activation (Srivastava *et al.*, 1998). Furthermore, another example of MT-dependent phosphorylation is known with NuMA protein (Nuclear Mitotic Apparatus protein) in mitotic HeLa cell extracts (Gaglio *et al.*, 1995).

We found that stathmin/Op18 hyperphosphorylation promoted by *Xenopus* permeabilized sperm heads, which possess both DNA and centrosomes, was prevented in the presence of nocodazole. This led us to propose that the previously observed effect of chromatin on stathmin/Op18 hyperphosphorylation was due to the chromatin-stabilized MTs, rather than to chromatin *per se* (Andersen *et al.*, 1997). We confirmed this directly using chromatin from somatic cells and showing that the associated hyperphosphorylating activity was abolished in the absence of MTs. Moreover, the recent demonstration of an involvement of Ran GTPase in MT nucleation during mitosis (Kahana and Cleveland, 1999) has led to the proposal that mitotic chromatin triggers MT assembly by regulating Ran activity (Kalab *et al.*, 1999; Carazo-Salas *et al.*, 1999). MTs assembled around chromatin could then induce the phosphorylation of stathmin/Op18 Ser 16. This would result in down-regulation of stathmin/Op18 MT destabilizing activity, thus favoring locally more MT assembly. Accordingly, immunodepletion experiments in egg extracts have shown that the activity of stathmin/Op18 by itself is not required to allow formation of the spindle (Andersen *et al.*, 1997), whereas in somatic cells its inactivation by extensive phosphorylation is required (Marklund *et al.*, 1996). The combination of both Ran-dependent and stathmin/Op18-dependent mechanisms would explain how MTs can assemble and then get stabilized by mitotic chromatin in egg extracts in the absence of centrosomes.

MT Assembly-dependent Phosphorylation Targets Stathmin/Op18 Ser 16

A basal phosphorylation on *Xenopus* stathmin/Op18 Ser 25 and Ser 39, which are the targets for cyclin-dependent kinases and MAP kinases, has already been shown in mitotic *Xenopus* egg extracts (Andersen *et al.*, 1997). We observed here that the MT assembly-dependent phosphorylation of stathmin/Op18 in mitotic and interphasic (our unpublished results) egg extracts is targeted to Ser16, which is not an MAP kinase or a p34^{cdc2} site. Our results suggest therefore

that the effect of MT assembly on stathmin/Op18 phosphorylation mainly consists in the activation of another kinase (or inhibition of a phosphatase), the target of which is Ser 16 on stathmin/Op18. Ser 16 is known to be a substrate *in vitro* and *in vivo* for Ca²⁺/calmodulin-dependent protein kinase type II (le Gouvello *et al.*, 1998) and type IV/Gr (Marklund *et al.*, 1994). The phosphorylation of this site is critical in the regulation of stathmin/Op18 MT-depolymerizing activity (Melander Gradin *et al.*, 1997; Gavet *et al.*, 1998), because observations in mammalian cells showed that phosphorylations on Ser 25 and Ser 38 (Ser 39 in *Xenopus*) have little effect on the activity of stathmin/Op18 (Larsson *et al.*, 1997), whereas additional phosphorylation of Ser 16 suppresses its MT-destabilizing effect (Melander Gradin *et al.*, 1997; Gavet *et al.*, 1998).

Physiological Relevance of the MT-dependent Stathmin/Op18 Hyperphosphorylation

The limited amount of stathmin/Op18 hyperphosphorylated following MT assembly raises the question of its physiological relevance (see above). We show here that the MT-dependent phosphorylation of stathmin/Op18 is involved in important biological events such as MT stabilization around chromatin in egg extracts (Figure 8). Moreover, our results could signify that stathmin/Op18 becomes locally phosphorylated in the vicinity of assembling MTs, consistent with observations in mammalian cells showing that phosphorylation on Ser 16 is more important around the mitotic spindle (Gavet *et al.*, 1998). This should not result in a dramatic increase of the most phosphorylated forms with respect to the total stathmin/Op18 pool. A similar situation has been reported for the activated forms of MAP kinases in mitosis, which are locally detected around the spindle with an anti-phosphoepitope antibody specific to active forms by immunofluorescence, but are hardly detected by Western blot (Shapiro *et al.*, 1998).

In addition, our observation that the time course of stathmin/Op18 phosphorylation upon MT assembly shows two characteristic times (Figure 5) suggests that the specific kinase/phosphatase responsible for stathmin/Op18 phosphorylation gets immediately into action, but that the hyperphosphorylated forms accumulate over time, and reach a steady-state level only after a lag of >15 min. Although the mechanisms responsible for this lag are unknown, we note that it corresponds to the time required for paclitaxel-induced aster formation (Gaglio *et al.*, 1995). This could mean that the organization of MTs in asters could also contribute to the hyperphosphorylation effect. As a matter of fact, we note that random tubulin autopolymerization frequent in interphase extracts is not sufficient to induce MT-dependent stathmin phosphorylation (Figure 3, lane C). Alternatively, this lag could be related to the tight cellular control of MT biogenesis that involves several, as yet poorly characterized factors (Solomon, 1991). Remarkably, most of the genes that have been found in yeast to affect MT-dependent processes, appear to affect MT polymerization only indirectly (Geissler *et al.*, 1998; Vega *et al.*, 1998, and references therein).

Stathmin/Op18 has been proposed to act as a relay in various transduction pathways for extracellular signals (Sobel, 1991), and to regulate the MT network (Belmont and Mitchison, 1996; Melander Gradin *et al.*, 1997; Gavet *et al.*, 1998; Melander Gradin *et al.*, 1998). Our results uncover a

new role of stathmin/Op18 in the integration of signals originating from the MT network itself, thus enabling auto-adaptation. Regulation of the steady-state level of polymerized tubulin, which is expected to require an overall negative feedback loop, probably requires many cooperating mechanisms that remain to be discovered but certainly involves capping proteins, MAPs, molecular motors, or factors not participating in the polymerization reaction itself but in other steps such as the formation of the α/β -tubulin dimers (Vega *et al.*, 1998). The positive feedback loop provided by stathmin/Op18 phosphorylation on Ser 16 represents an additional mechanism for MT network control. It should enable transitions of global MT dynamics in response to variations in cellular conditions, for example in response to extracellular signals or in the interphase to mitosis transition, but might also act locally within the cell at any time.

ACKNOWLEDGMENTS

We thank S. Middendorp and M. Moudjou for help in HeLa cell experiments; A. Paoletti and A. Rousselet for introduction to *Xenopus* cell extracts; E. Bailly for suggesting experiments; and Y. Abraham, B. Fiévet, and A. Maucuer for help in quantitation experiments. M. Lohka, D. Cleveland, M. Piel, and S. Holmes are acknowledged for stimulating discussions. We are grateful to D. Morineau and D. Meur for artwork, and to G. Keryer, S. Holmes, V. Doye, and E. Charbaut for critical reading of the manuscript. T.K. received fellowships from the Ministère de l'Enseignement Supérieur et de la Recherche, from Association pour la Recherche sur le Cancer and from the Luxembourg Ministère de l'Education Nationale et de la Formation Professionnelle during this work. O.G. received a fellowship from the Ligue Nationale contre le Cancer. This work was supported by Center National de la Recherche Scientifique, Institut Curie and by a European Economic Community Grant HCP CHRX CT 94-0642 to M.B.

REFERENCES

- Andersen, S.S., Ashford, A.J., Tournebize, R., Gavet, O., Sobel, A., Hyman, A.A., and Karsenti, E. (1997). Mitotic chromatin regulates phosphorylation of Stathmin/Op18. *Nature* 389, 640–643.
- Belmont, L.D., and Mitchison, T.J. (1996). Identification of a protein that interacts with tubulin dimers and increases the catastrophe rate of microtubules. *Cell* 84, 623–631.
- Beretta, L., Dobransky, T., and Sobel, A. (1993). Multiple phosphorylation of stathmin. Identification of four sites phosphorylated in intact cells and in vitro by cyclic AMP-dependent protein kinase and p34cdc2. *J. Biol. Chem.* 268, 20076–20084.
- Bornens, M. (1968). Méthode d'isolement de la membrane nucléaire de foie de rat. *C. R. Acad. Sci.* III 266, 596–599.
- Bornens, M., and Moudjou, M. (1999). Studying the composition and function of centrosomes in vertebrates. In: *Methods in Cell Biology*, vol 61, ed. C.L. Rieder, New York: Academic Press, 13–34.
- Brattsand, G., Marklund, U., Nylander, K., Roos, G., and Gullberg, M. (1994). Cell-cycle-regulated phosphorylation of oncoprotein 18 on Ser16, Ser25 and Ser38. *Eur. J. Biochem.* 220, 359–368.
- Carazo-Salas, R.E., Guarguaglini, G., Gruss, O.J., Segref, A., Karsenti, E., and Mattaj, I.W. (1999). Generation of GTP-bound Ran by RCC1 is required for chromatin-induced mitotic spindle formation. *Nature* 400, 178–181.
- Curmi, P.A., Andersen, S.S., Lachkar, S., Gavet, O., Karsenti, E., Knossow, M., and Sobel, A. (1997). The stathmin/tubulin interaction in vitro. *J. Biol. Chem.* 272, 25029–25036.
- Gaglio, T., Saredi, A., and Compton, D.A. (1995). NuMA is required for the organization of microtubules into aster-like mitotic arrays. *J. Cell Biol.* 131, 693–708.
- Gavet, O., Ozon, S., Manceau, V., Lawler, S., Curmi, P., and Sobel, A. (1998). The stathmin phosphoprotein family: intracellular localization and effects on the microtubule network. *J. Cell Sci.* 111, 3333–3346.
- Geissler, S., Siegers, K., and Schiebel, E. (1998). A novel protein complex promoting formation of functional α - and γ -tubulin. *EMBO J.* 17, 952–966.
- Gigant, B., Curmi, P.A., Martin-Barbey, C., Charbaut, E., Lachkar, S., Lebeau, L., Siavoshian, S., Sobel, A., and Knossow, M. (2000). The 4 140 X-ray structure of a tubulin:stathmin-like domain complex. *Cell* 102, 809–816.
- Horwitz, S.B., Shen, H.J., He, L., Dittmar, P., Neef, R., Chen, J., and Schubart, U.K. (1997). The microtubule-destabilizing activity of metablastin (p19) is controlled by phosphorylation. *J. Biol. Chem.* 272, 8129–8132.
- Howell, B., Deacon, H., and Cassimeris, L. (1999a). Decreasing oncoprotein 18/stathmin reduces microtubules catastrophes and increases microtubule polymer in vivo. *J. Cell Sci.* 112, 3713–3722.
- Howell, B., Larsson, N., Gullberg, M., and Cassimeris, L. (1999b). Dissociation of the tubulin-sequestering and microtubule catastrophe-promoting activities of oncoprotein 18/Stathmin. *Mol. Biol. Cell* 10, 105–118.
- Jourdain, L., Curmi, P., Sobel, A., Pantaloni, D., and Carlier, M.F. (1997). Stathmin: a tubulin-sequestering protein which forms a ternary T2S complex with two tubulin molecules. *Biochemistry* 36, 10817–10821.
- Kahana, J.A., and Cleveland, D.W. (1999). Beyond nuclear transport. Ran-GTP as a determinant of spindle assembly. *J. Cell Biol.* 146, 1205–1210.
- Kalab, P., Pu, R.T., and Dasso, M. (1999). The Ran GTPase regulates mitotic spindle assembly. *Curr. Biol.* 9, 481–484.
- Koppel, J., Boutterin, M.C., Doye, V., Peyro-Saint-Paul, H., and Sobel, A. (1990). Developmental tissue expression and phylogenetic conservation of stathmin, a phosphoprotein associated with cell regulations. *J. Biol. Chem.* 265, 3703–3707.
- Laemmli, U.K. (1970). Cleavage of structural proteins during the assembly of the head of bacteriophage T4. *Nature* 227, 680–685.
- Larsson, N., Marklund, U., Melander Gradin, H., Brattsand, G., and Gullberg, M. (1997). Control of microtubule dynamics by oncoprotein 18: dissection of the regulatory role of multisite phosphorylation during mitosis. *Mol. Cell. Biol.* 17, 5530–5539.
- Larsson, N., Segerman, B., Howell, B., Fridell, K., Cassimeris, L., and Gullberg, M. (1999). Op18/stathmin mediates multiple region-specific tubulin and microtubule-regulating activities. *J. Cell Biol.* 146, 1289–1302.
- Lawler, S., Gavet, O., Rich, T., and Sobel, A. (1998). Stathmin overexpression in 293 cells affects signal transduction and cell growth. *FEBS Lett.* 421, 55–60.
- le Gouvello, S., Manceau, V., and Sobel, A. (1998). Serine 16 of stathmin as a cytosolic target for Ca²⁺/calmodulin-dependent kinase II after CD2 triggering of human T lymphocytes. *J. Immunol.* 161, 1113–1122.
- Luo, X.N., Mookerjee, B., Ferrari, A., Mistry, S., and Atweh, G.F. (1994). Regulation of phosphoprotein p18 in leukemic cells. Cell cycle regulated phosphorylation by p34cdc2 kinase. *J. Biol. Chem.* 269, 10312–10318.
- Marklund, U., Larsson, N., Brattsand, G., Osterman, G., Chatila, T.A., and Gullberg, M. (1994). Serine 16 of oncoprotein 18 is a major

- cytosolic target for the Ca²⁺/Calmodulin-dependent kinase-Gr. *Eur. J. Biochem.* *225*, 53–60.
- Marklund, U., Larsson, N., Melander Gradin, H., Brattsand, G., and Gullberg, M. (1996). Oncoprotein 18 is a phosphorylation-responsive regulator of microtubule dynamics. *EMBO J.* *15*, 5290–5298.
- Maucuer, A., Moreau, J., Mechali, M., and Sobel, A. (1993). Stathmin gene family: phylogenetic conservation and developmental regulation in *Xenopus*. *J. Biol. Chem.* *268*, 16420–16429.
- Melander Gradin, H., Larsson, N., Marklund, U., and Gullberg, M. (1998). Regulation of microtubule dynamics by extracellular signals: cAMP-dependent protein kinase switches off the activity of Oncoprotein 18 in intact cells. *J. Cell Biol.* *140*, 131–141.
- Melander Gradin, H., Marklund, U., Larsson, N., Chatila, T.A., and Gullberg, M. (1997). Regulation of microtubule dynamics by Ca²⁺/calmodulin-dependent kinase IV/Gr-dependent phosphorylation of oncoprotein 18. *Mol. Cell. Biol.* *17*, 3459–3467.
- Mirsky, A.E., and Pollister, A.W. (1946). Chromosin, a desoxyribose nucleoprotein complex of the cell nucleus. *J. Gen. Physiol.* *30*, 101–116.
- Morishima-Kawashima, M., and Kosik, K.S. (1996). The pool of MAP kinase associated with microtubules is small but constitutively active. *Mol. Biol. Cell* *7*, 893–905.
- Moudjou, M., Bordes, N., Paintrand, M., and Bornens, M. (1996). γ -tubulin in mammalian cells: the centrosomal and the cytosolic forms. *J. Cell Sci.* *109*, 875–887.
- Murray, A.W. (1991). Cell cycle extracts. *Methods Cell Biol.* *36*, 581–605.
- Ohta, Y., Ohba, T., and Miyamoto, E. (1990). Ca²⁺/calmodulin-dependent protein kinase II: localization in the interphase nucleus and the mitotic apparatus of mammalian cells. *Proc. Natl. Acad. Sci. USA* *87*, 5341–5345.
- Ookata, K., Hisanaga, S., Okumura, E., and Kishimoto, T. (1993). Association of p34cdc2/cyclin B complex with microtubules in starfish oocytes. *J. Cell Sci.* *105*, 873–881.
- Reszka, A.A., Seger, R., Diltz, C.D., Krebs, E.G., and Fischer, E.H. (1995). Association of mitogen-activated protein kinase with the microtubule cytoskeleton. *Proc. Natl. Acad. Sci. USA* *92*, 8881–8885.
- Sawin, K.E., and Mitchison, T.J. (1991). Mitotic spindle assembly by two different pathways in vitro. *J. Cell Biol.* *112*, 925–940.
- Shapiro, P.S., Vaisberg, E., Hunt, A.J., Tolwinski, N.S., Whalen, A.M., McIntosh, J.R., and Ahn, N.G. (1998). Activation of the MKK/ERK pathway during somatic cell mitosis: direct interactions of active ERK with kinetochores and regulation of the mitotic 3F3/2 phosphoantigen. *J. Cell Biol.* *142*, 1533–1545.
- Shinohara-Gotoh, Y., Nishida, E., Hoshi, M., and Sakai, H. (1991). Activation of microtubule-associated protein kinase by microtubule disruption in quiescent rat 3Y1 cells. *Exp. Cell Res.* *193*, 161–166.
- Sobel, A. (1991). Stathmin: a relay phosphoprotein for multiple signal transduction? *Trends Biochem. Sci.* *16*, 301–305.
- Sobel, A., Bouterin, M.C., Beretta, L., Chneiweiss, H., Doye, V., and Peyro-Saint-Paul, H. (1989). Intracellular substrates for extracellular signaling. Characterization of a ubiquitous, neuron-enriched phosphoprotein (stathmin). *J. Biol. Chem.* *264*, 3765–3772.
- Sobel, A., and Tashjian, A.H., Jr. (1983). Distinct patterns of cytoplasmic protein phosphorylation related to regulation of synthesis and release of prolactin by GH cells. *J. Biol. Chem.* *258*, 10312–10324.
- Solomon, F. (1991). Analysis of the cytoskeleton in *Saccharomyces cerevisiae*. *Annu. Rev. Cell Biol.* *7*, 633–662.
- Sontag, E., Nunbhakdi-Craig, V., Bloom, G.S., and Mumby, M.C. (1995). A novel pool of protein phosphatase 2A is associated with microtubules and is regulated during the cell cycle. *J. Cell Biol.* *128*, 1131–1144.
- Srivastava, R.K., Srivastava, A.R., Korsmeyer, S.J., Nesterova, M., Cho-Chung, Y.S., and Longo, D.L. (1998). Involvement of microtubules in the regulation of Bcl2 phosphorylation and apoptosis through cyclic AMP-dependent protein kinase. *Mol. Cell Biol.* *18*, 3509–3517.
- Steinmetz, M.O., Kammerer, R.A., Jahnke, W., Goldie, K.N., Lustig, A., and van Oostrum, J. (2000). Op18/stathmin caps a kinked protofilament-like tubulin tetramer. *EMBO J.* *19*, 572–580.
- Strahler, J.R., Lamb, B.J., Ungar, D.R., Fox, D.A., and Hanash, S.M. (1992). Cell cycle progression is associated with distinct patterns of phosphorylation of Op18. *Biochem. Biophys. Res. Commun.* *185*, 197–203.
- Tournebize, R., Andersen, S.S., Verde, F., Doree, M., Karsenti, E., and Hyman, A.A. (1997). Distinct roles of PP1 and PP2A-like phosphatases in control of microtubule dynamics during mitosis. *EMBO J.* *16*, 5537–5549.
- Vega, L.R., Fleming, J., and Solomon, F. (1998). An α -tubulin mutant destabilizes the heterodimer: phenotypic consequences and interactions with tubulin-binding proteins. *Mol. Biol. Cell* *9*, 2349–2360.